Neuropharmacology 60 (2011) 1176–1186

Contents lists available at ScienceDirect

Neuropharmacology

journal homepage: www.elsevier.com/locate/neuropharm

Functional reduction of SK3-mediated currents precedes AMPA-receptor-mediated excitotoxicity in dopaminergic neurons

Bruno A. Benítez [a], Helen M. Belálcazar [a], Agustín Anastasía [b], Daniel T. Mamah [b], Charles F. Zorumski [b], Daniel H. Mascó [b], Daniel G. Herrera [a], Gabriel A. de Erausquin [a,*]

[a] Laboratory of Brain Development, Modulation and Repair, Brigham and Women's Hospital, Harvard Medical School, MA, USA
[b] Department of Psychiatry, Washington University School of Medicine, MO, USA

ARTICLE INFO

Article history:
Received 1 August 2010
Received in revised form
28 September 2010
Accepted 26 October 2010

Keywords:
Dopaminergic
SK channels
Apamin
1-Ebio
CyPPA
NS8593 AMPA
Excitotoxicity
Neuroprotection

ABSTRACT

In primary cultures of mesencephalon small-conductance calcium-activated potassium channels (SK) are expressed in dopaminergic neurons. We characterized SK-mediated currents (I_{SK}) in this system and evaluated their role on homeostasis against excitotoxicity. I_{SK} amplitude was reduced by the glutamatergic agonist AMPA through a reduction in SK channel number in the membrane. Blockade of I_{SK} for 12 h with apamin or NS8593 reduced the number of dopaminergic neurons in a concentration-dependent manner. The effect of apamin was not additive to AMPA toxicity. On the other hand, two I_{SK} agonists, 1-EBIO and CyPPA, caused a significant reduction of spontaneous loss of dopaminergic neurons. 1-EBIO reversed the effects of both AMPA and apamin as well. Thus, I_{SK} influences survival and differentiation of dopaminergic neurons *in vitro*, and is part of protective homeostatic responses, participating in a rapidly acting negative feedback loop coupling calcium levels, neuron excitability and cellular defenses.

This article is part of a Special Issue entitled 'Trends in Neuropharmacology: In Memory of Erminio Costa'.

1. Introduction

A stereotypical pattern of differential neuronal dysfunction or death of specific subgroups of dopaminergic neurons (DN) has been implicated in a broad array of neurologic and psychiatric disorders, especially in Parkinson's disease (Moore et al., 2005) and schizophrenia (de Erausquin and Hanbauer, 1995; Yang et al., 1999). Intricate spatiotemporal patterns of dopaminergic dysfunction are reproducible among multiple *in vitro* (Dauer and Przedborski, 2003) and *in vivo* (Damier et al., 1999) experimental models. However, the involved molecular mechanisms remain an unsolved puzzle (Harrison and Weinberger, 2005; Licker et al., 2009).

DN show a singular, stereotyped and well-defined electrophysiological phenotype, which confers them a functional identity in tissue slices (Grace and Bunney, 2000) as well as in primary cultures (Chiodo and Kapatos, 1992). Intrinsic electrical properties of DN are functionally correlated with differential expression and assembly of ion channels and their subcellular distribution (Liss and Roeper, 2008); in fact, intrinsic excitability and the patterns of activity of DN are tightly regulated by A-type K^+-channels (Kv4.3/Kchip3.1 K) (Liss et al., 2001), G-protein coupled potassium (GIRK2) channels (Beckstead et al., 2004), voltage-gated L-type calcium channels (Cav1.3) (Puopolo et al., 2007), hyperpolarization-activated cyclic nucleotide-gated cation (HCN) channels (Neuhoff et al., 2002; Seutin et al., 2001) SK channels (Ji and Shepard, 2006), and ATP-sensitive potassium (K-ATP) channels (Kir6.2 and SUR1 subunits) (Liss et al., 2005). More to the point of this communication, cell-to-cell variability of kinetic properties, spatial distribution, or abundance of sets of ion channels underlies substantial differences in determination of cell fate (Michel et al., 2007). Thus, in the case of DN, Cav1.3 channels (Chan et al., 2007) and K-ATP channels (Liss et al., 2005) have been shown to

Abbreviations: SK, small-conductance calcium-activated potassium channels; I_{SK}, SK channel-mediated current; I_{AHP}, afterhyperpolarization; VDCC, voltage-dependent calcium channels; STN, subthalamic nucleus; TH, tyrosine hydroxylase; DN, dopaminergic neurons; PD, Parkinson disease; AMPA, alpha-amino-3-hydroxy-5-methyl-4-isoxazolepropionic-Acid; 1-EBIO, 1-ethyl-2-benzimidazolinone; NS8593, (R)-N-(benzimidazol-2-yl)-1,2,3,4-tetrahydro-1-naphtylamine; CyPPA, N-cyclohexyl-N-[2-(3,5-dimethyl-pyrazol-1-yl)-6-methyl-4-pyrimidinamine; 4-AP, 4-aminopyridine; TEA, tetraethylammonium; TTX, tetrodotoxin; NMDA, N-methyl-d-aspartate; SNpc, substantia nigra pars compacta; CREB, c-AMP responsive element binding protein.

* Corresponding author. Harvard Institutes of Medicine, #921C, 77 Ave. Louis Pasteur, Boston, MA 02115, USA. Tel.: +1 617 525 5060; fax: +1 617 525 5067.
E-mail address: gdeerausquin@partners.org (G.A. de Erausquin).

0028-3908/$ – see front matter © 2010 Elsevier Ltd. All rights reserved.
doi:10.1016/j.neuropharm.2010.10.024

determine distinct subsets of neurons with differential susceptibility to degeneration (Liss and Roeper, 2008).

SK channels are activated by small increases in intracellular calcium concentration and are responsible for the apamin-sensitive afterhyperpolarization current, I_{AHP} (Bond et al., 2004); these channels are an ideally suited feedback system to regulate the spatiotemporal occurrence of calcium transients in microdomains near the cellular membrane (Fakler and Adelman, 2008). Activation of SK channels suppresses hyperexcitability induced by a range of depolarizing agents (Lappin et al., 2005; Garduno et al., 2005; Kobayashi et al., 2008). Likewise, over-expression of the dominant-inhibitory construct SK3-1B results in hyperexcitability without neurodegeneration (Shakkottai et al., 2004). On the other hand, over-expression of SK channels prevents kainate and glutamate-induced excitotoxicity, enhancing survival of cortical neurons *in vitro* and *in vivo* (Lee et al., 2003). Lastly, and closest to the results analyzed in this report, pharmacological activation of SK channels *in vivo* increases survival of DN subjected to a selective neurodegeneration challenge (Aumann et al., 2008). Taken together, the data suggest that SK channels may be part of first line protective homeostatic responses in neurons, participating in a rapidly acting negative feedback loop coupling calcium levels, neuron excitability and cellular defenses against excitotoxic insults (Tanabe et al., 1999; Sapolsky, 2001).

DN respond to glutamate-induced depolarization with a short latency hyperpolarization (I_{AHP}) mediated in part by SK channel activation, followed by a sustained depolarization when I_{SK} becomes inactive (Fiorillo and Williams, 1998). In midbrain DN in slices, glutamate activates an SK-mediated I_{AHP} through metabotropic glutamate receptors triggered calcium release from intracellular stores (Fiorillo and Williams, 1998). However, sustained exposure to glutamate desensitizes this response and results in depolarization (Fiorillo and Williams, 1998). Given that sustained activation of AMPA ionotropic glutamate receptors leads to loss of calcium homeostasis in embryonic DN also through a mechanism requiring calcium-induced calcium release from intracellular stores (de Erausquin et al., 1994a, 1994b), an intriguing possibility is that glutamate-induced suppression of SK-mediated I_{AHP} in DN may be a required step to express the susceptibility of DN to glutamate toxicity.

Primary cultures of embryonic mesencephalon are a widely used and well-characterized tool to investigate molecular mechanisms involved in the development, maintenance, differentiation and death of DN (Branton and Clarke, 1999; Falkenburger and Schulz, 2006). Most of the molecular processes involved in the specification of neuronal identity, maturation and differentiation of DN have been established in this system (Alavian et al., 2008). DN in culture show a mature functional signature similar, but not identical, to that found *in vivo* or in slice preparations (Greco et al., 2009; Chiodo and Kapatos, 1992; Liss et al., 2001; Neuhoff et al., 2002; Seutin et al., 2001), and therefore represent an imperfect but well established model of the adult phenotype. In this simplified system, we established that protracted stimulation of AMPA receptors results in phenotype-specific toxicity to a subpopulation of DN (de Erausquin et al., 1994a, 2003; Isaacs et al., 1996; Dorsey et al., 2006). Also, we have previously shown that direct application of NMDA is not toxic to cultured DN (Isaacs et al., 1996), and fails to induce significant changes in intracellular free calcium concentrations or increase phosphorylation of c-AMP responsive element binding protein (CREB) in the same system (de Erausquin et al., 1994a). Thus, rather than an accurate model of excitotoxicity to DN in neurodegenerative diseases, AMPA-induced death may resemble ontogenetically regulated natural cell death of DN (Burke, 2004) and the mechanism by which susceptible populations are affected in psychiatric neurodevelopmental disorders (de Erausquin and Hanbauer, 1995). Indeed, primary cultures are plated during a critical period of the ontogeny of excitatory glutamatergic circuitry between STN and SNpc in which AMPA receptors reach the peak of expression at the midbrain (Lilliu et al., 2001) and glutamatergic projections from STN reach the SNpc (Marani et al., 2008).

We now tested the hypothesis that differential susceptibility of DN to stimulation of AMPA receptors depends upon effects on its electrophysiological signature; in particular, we tested if I_{SK} plays a neuroprotective role against AMPA-receptor-mediated excitotoxicity to DN.

2. Materials and methods

2.1. Animals and dissections

Animals were treated in accordance with the National Institutes of Health Guide for the Care and Use of Laboratory Animals. Brigham and Women's animal experimentation committee approved all procedures. Primary cultures were established from ventral mesencephalon of rat embryos as described previously (de Erausquin et al., 1994a, 2003; Isaacs et al., 1996). Briefly, timed-pregnant Sprague–Dawley rats (Charles River Laboratories, MA, USA) were exposed to CO_2 on day 14 of gestation and following laparotomy embryos were quickly removed and placed in cold Hanks' Balanced Salt Solution (Sigma–Aldrich, MO, USA). Under a stereoscope (Nikon SMZ-1B, 100× magnification), brains were dissected, brainstems isolated and meninges carefully removed. Approximately 1.0-mm^3 blocks of tissue were isolated from the ventral mesencephalon.

2.2. Cell cultures

Dissected tissue blocks were triturated with ~15 strokes of a flame-constricted Pasteur pipette in 3 ml of Dulbecco Modified Eagle's Medium/HAM F12 (DMEM/F12) (Sigma–Aldrich, MO, USA). Cells were then suspended at a density of 10×10^5/ml in plating medium (50/50 DMEM/F12) (Sigma–Aldrich, MO, USA) with 15 mM N-2-Hydroxyethylpiperazine-N′-2′-ethanesulfonic Acid (HEPES), glucose (25 mM), glutamine (2 mM), 10% horse serum, basic Fibroblast Growth Factor (bFGF) (10 ng/ml) and penicillin and streptomycin (10 U/ml and 10 mg/ml, respectively). An aliquot of 150 μL was plated onto on glass coverslip-bottom 35 mm dishes (MatTek Corporation) pre-coated with poly-D-lysine (15 μg/ml) (Sigma–Aldrich, MO, USA) and laminin (10 μg/ml) (Invitrogen, USA); dishes were incubated at 37 °C in 5% CO_2 at 100% humidity for 1 h to allow the cells to attach to the coated surface. Toxicity experiments were done on 24-well plastic plates pre-coated with poly-D-lysine (15 μg/ml) (Sigma–Aldrich, MO, USA) and laminin (10 μg/ml) (Invitrogen, USA) at a density of 2.0×10^5 cells. Differentiation was induced after 3 days *in vitro* (DIV) replacing the culture medium by a serum-free medium containing Neurobasal medium (Invitrogen, USA) supplemented with 2% B27 (Invitrogen, USA) and Glutamax 0.5 mM (Invitrogen, USA). Culture medium was renewed every 48 h. Experiments were done after 7–11 DIV (de Erausquin et al., 1994a, 2003; Isaacs et al., 1996). Cultures were grown at 37 °C in an atmosphere of 5% CO_2/95% air and 100% relative humidity.

2.2.1. Pharmacological treatments

Cells were exposed to alpha-Amino-3-hydroxy-5-methyl-4-isoxazolepropionic-Acid (AMPA) (3–1000 μM), apamin (3–1000 nM), 1-ethyl-2-benzimidazolinone (1-EBIO) (3–1000 μM), (R)-N-(benzimidazol-2-yl)-1,2,3,4-tetrahydro-1-naphtylamine (NS8593) (0.03–10 μM), N-Cyclohexyl-N-[2-(3,5-dimethyl-pyrazol-1-yl)-6-methyl-4-pyrimidinamine (CyPPA) (0.03–10 μM) for 12 h (DIV 10–11). Treatments were stopped by rinsing briefly with PBS, then fixing for TH immunocytochemistry. For experiments, alls drugs were dissolved in the extracellular solution in concentrations as indicated. Apamin, NS8593, 4-Aminopyridine (4-AP), and tetraethylammonium (TEA) were obtained from Sigma–Aldrich, MO, USA. AMPA, 1-EBIO, Tetrodotoxin (TTX), and CyPPA were from (Tocris Bioscience, MO, USA).

2.2.2. Immunohistochemical procedure

Cultures were fixed at ice-cold 4% paraformaldehyde in PBS fresh prepared, permeabilized in 0.25% Triton-X 100 (Sigma–Aldrich, MO, USA) for 10 min, and blocked by incubation in 10% goat serum. Cultures were incubated in the primary antibody tyrosine hydroxylase (TH) 1:500 diluted (Peel freeze, AR, USA) or SK3 channels 1:150 (Alomone labs, Jerusalem, Israel) for 16 h at 4 °C, followed by secondary antibodies conjugated to Alexa-488 (1:200) or Alexa-568 (1:200) (Molecular Probes, Eugene, Oregon) for 2 h, room temperature, or peroxidase conjugated (Sigma–Aldrich, MO, USA). Controls were stained omitting the primary or secondary antibody. Specimens were examined and photographed on an inverted microscope fitted with a (Nikon Diaphot, with a Nikon Apo 20× dry objective, 75 W xenon lamp, rhodamine and fluorescene filters, cooled CCD camera – SPOT 32, Diagnostic Instruments Inc.), and analyzed (ImageJ, NIH, USA).

2.2.3. Cell counting and assessment of neuronal survival

The number of surviving neurons was determined by immunostaining as described previously (de Erausquin et al., 1994a, 2003; Isaacs et al., 1996). Neurons stained with anti-TH antibody were counted as positive when the cytosol and proximal dendrites were clearly filled with the fluorophore. The number of surviving TH-positive neurons was counted and normalized to the number of TH cells in untreated cultures. The number of TH-positive neurons was determined by counting 20 successive, contiguous microscopic fields, along diameters across each well. The total number of cells counted in each experiment, typically in the range of 150–300 cells per treatment, was counted in a blind-treated manner using an inverted microscope (Nikon Diaphot, Nikon Apo 20× dry objective; Nikon, Tokyo, Japan).

2.2.4. Morphology and quantization of neurites

Digital images of 10–15 microscopic fields containing at least one DN were captured (Nikon Diaphot, Nikon Apo 20× dry objective, 75 W xenon lamp, rhodamine and fluorescein filters, cooled CCD camera – SPOT 32, Diagnostic Instruments Inc.), and analyzed (ImageJ, NIH, USA). Cell process number, length and branch frequency were counted semi automatically; lengths were measured in pixels using a freehand mouse, transformed to μm using standard rulers, and averaged for each cell (NeuronJ, NIH, USA).

2.3. Electrophysiology

Patch-clamp measurements were performed in the whole-cell mode of the patch-clamp technique using standard methods. I_{AHP} was studied using the protocol introduced by Wolfart et al. (2001). Membrane voltage was stepped from a holding potential of −60 mV to a depolarized potential (+60 mV) for 100 ms to elicit a robust calcium influx corresponding to the generation of one or more all-or-none calcium spikes.

Pipette series resistance was 5 ± 2 MΩ when filled with intracellular solution containing (in mM): KCl, 150; EGTA, 0.1; and HEPES, 2 and Alexa Fluor 488 (80 μM, Molecular Probes, Eugene, OR). For experiments culture medium was replaced by an extracellular solution containing (in mM): NaCl, 138; KCl, 4; $CaCl_2$, 2; $MgCl_2$, 1; HEPES, 10; and glucose, 10. All recordings were made containing a noncompetitive antagonist at gamma amino butyric acid (GABA) A receptors (100 μM picrotoxin) and a noncompetitive antagonist at the glycine site of NMDA receptor (50 μM kynurenic acid) added. The pH of both solutions was adjusted to 7.25. Intracellular pipette solutions with low calcium-buffering capacity (0.1 mM EGTA) were used to minimize non-physiological calcium buffering (Wolfart et al., 2001). TTX (0.5 μM) and TEA (1 mM) (Pedarzani et al., 2005) were added to the extracellular medium to block sodium channels and large conductance calcium-sensitive (BK), M, and delayed rectifier potassium channels to make recordings for fluctuations analysis. Test solutions were freshly prepared before each experiment and were filtered through a 2-μm filter (Millipore, USA) prior to use. Access and input resistances were monitored throughout the recordings and cells were discarded if either value changed by more than 25% during the recording period (typically 15–30 min). Data are reported without corrections for liquid junction potentials. Patch pipettes were pulled from borosilicate glass (World Precision Instruments) with a Flaming/Brown micropipette puller (P-87 Model, Sutter Instrument, CA, USA). Open-tip pipette resistance in the bath was typically between 4 and 7 MΩ. All experiments were performed at room temperature (20–22 °C). After 7–11 days in culture, cells were pretreated 2 h with AMPA (100 mM) or apamin (20–100 nM) where stated, 1-EBIO (100 μM) was added to the bath. After patch-clamp experiments, mesencephalic cell cultures were fixed for 20 min in ice-cold 4% paraformaldehyde in PBS. Patch pipettes were filled with Alexa Fluor 488; counterstaining of a limited number of cells confirmed DN identity with anti-TH antibody. Except when noted, drugs were obtained from Sigma (St. Louis, MO). All Alexa Fluor reagents were from Invitrogen/Molecular Probes (Carlsbad, CA).

2.3.1. Data acquisition, storage, and analysis

Whole-cell recordings were made using a patch-clamp amplifier (Axo-patch 200B, Axon Instruments, CA, USA), filtered at 5 kHz, digitized using a 16-bit analog/digital converter (Digidata 1322, Axon Instruments), and stored on a PC running acquisition software (pClamp 8.2, Axon Instruments). Holding potential was clamped to −60 mV. Rise time was measured as the time needed for the current rise from 10 to 90% of amplitude maximum. Decay Time constants were measured by fitting curves with a first-order exponential function using Marquardt–Levenberg nonlinear least-squares algorithm (Clampfit 9.01, Axon Instruments, CA, USA). The charge transfer was measured using Clampfit 9.01 (Axon Instruments, CA, USA) by integrating the area under the current response trace, starting at the beginning of the response and finishing at the time when the current decayed by 90%.

2.3.1.1. Mean current–variance analysis. Mean current–variance analysis was carried out based in standard protocol (Sah and Isaacson, 1995; Valiante et al., 1997; Vogalis et al., 2001). In brief, to construct mean current–variance curves from the same cell, 10–15 individual I_{AHP} currents of stable amplitude were filtered at 10 Hz to obtain the current time course. Thus, 100 ms were sufficient to allow the decay of most of I_{AHP} to baseline. The traces selected were fitted using a least-square curve-fitting program (Clampfit in pCLAMP 9.0 or Graphpad Prism). This entailed fitting the raw current trace with a polynomial curve (or mean current) that was subtracted from each raw I_{AHP} current to obtain the difference current. These residuals were binned into several nonoverlapping intervals of 2 ms, and the variance was calculated for each bin. The variance (σ^2) was then calculated in each interval and the baseline variance subtracted. Binned variance was then averaged for all the 10–15 traces and plotted against the mean current in each interval. By partitioning the I_{AHP} decay into many subintervals, where the change in mean current is small, we could obtain a plot of σ^2 as a function of mean current to which we could fit the following equation (Sigworth, 1980; Heinemann and Conti, 1992):

$$\sigma^2 = i^*I_{mean} - (I_{mean})2/N \quad (1)$$

to obtain estimates for i, which is equal to the single-channel current, and N, which represents the maximum number of channels in the cell. I_{mean} is the mean whole-cell current.

2.4. Statistical analysis

Each experiment was performed with at least three different batches of neurons, and toxicity assays were repeated at least three times for each batch. Results are represented as mean ± SEM. Data were analyzed using GraphPad Prism (version 5.00 for Windows, GraphPad Software, CA, USA). Statistical analysis was performed by Kolmogorov–Smirnov normality test. Paired and unpaired statistical comparisons were made using the two-tailed student's *T* test with a 95% confidence interval. For statistical comparison involving multiple groups, one-way ANOVA followed by post-hoc Tukey multiples comparison test was performed. *p* Values of <0.05 were used as the criterion for determining statistically significant differences.

3. Results

3.1. SK3 channels are expressed in a subpopulation of cultured DN

SK channels exist on several isoforms of which, at least *in vivo*, DN express preferentially the SK3 variant (Stocker and Pedarzani, 2000). No published information is currently available on the expression of SK3 channels in embryonic primary cultures of mesencephalon. We carried out double labeling for TH and SK3 in 7–10 DIV cultures. SK3-positive neurons showed two majors morphologies; most frequently observed were fusiform to spindle-shaped bipolar neurons with small somas and 2–3, rarely branched, primary dendrites (Fig. 1A). Multipolar neurons with large somas and 3–6 tapering primary dendrites with multiple terminal branches were also found (Fig. 1G). At 10 DIV, SK3-positive neurons showed strong co-immunoreactivity for TH (Fig. 1C), but we virtually never found SK3 immunoreactivity in TH-negative (i.e., non-dopaminergic) neurons. On the other hand, only a subpopulation of TH-positive cells showed SK3 colocalization (Fig. 1F). That is to say, SK3 expression is found almost exclusively in DN in this preparation, even though SK3-expressing neurons represent only a fraction of the total complement of DN.

Most SK3 staining was found on the soma and proximal neurites (Fig. 1G). TH-positive axons generally started as a typical dendrite with gradually decreasing diameter, continued as a thin process of an almost constant diameter. Rarely, the axon departed directly from the soma or from the proximal part of a primary dendrite. When identified, the thin, untapering axons were clearly longer than dendrites (Fig. S1). These findings are in agreement with published data showing SK3 mRNA and protein levels highly expressed in adult DA midbrain neurons, with highest levels in SNpc (Stocker and Pedarzani, 2000; Tacconi et al., 2001; Sarpal et al., 2004), where they have a somatodendritic distribution (Wolfart et al., 2001).

3.2. Properties of I_{AHP} in cultured DN

The presence of I_{AHP} identifies DN in primary cultures of embryonic (Chiodo and Kapatos, 1992) or postnatal mesencephalon (Silva et al., 1990), but virtually nothing is known about the role of SK channels in its production in these systems. We performed whole-cell somatic voltage-clamp recordings from e14 primary cultures

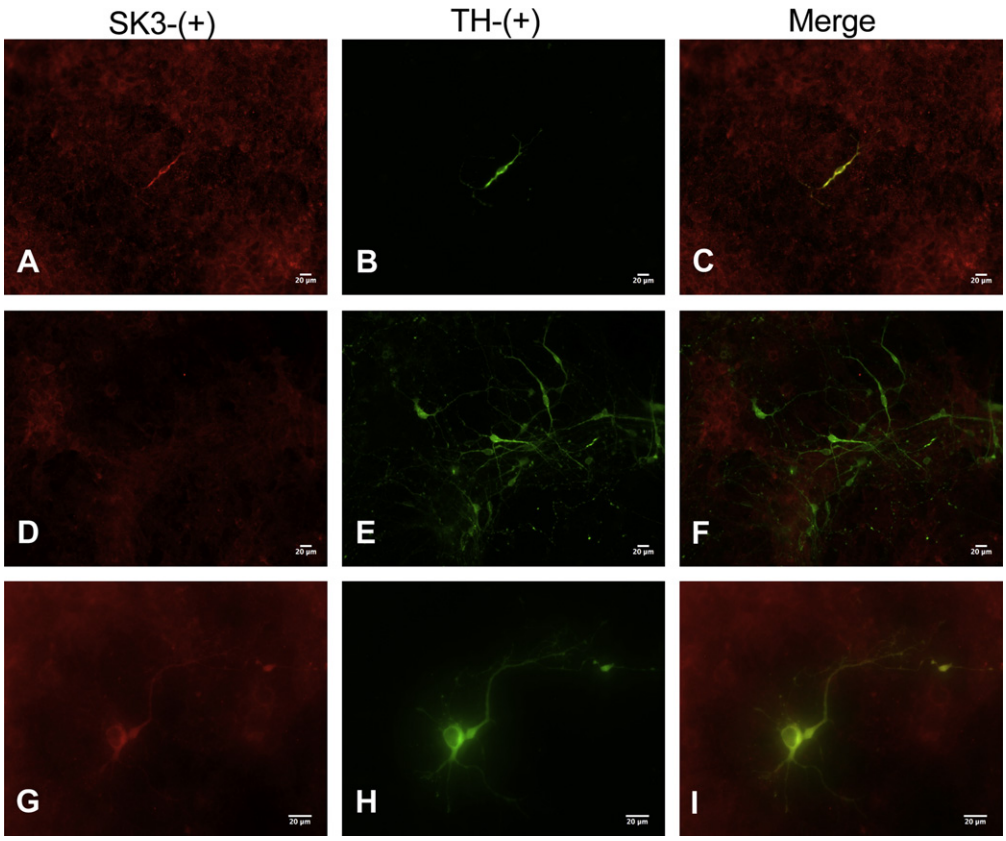

Fig. 1. Double immunofluorescence labeling of cultured embryonic rat ventral mesencephalon neurons with antibodies against SK3 and TH. Anti-SK3 antibody labeled two populations of SK3-positive neurons: fusiform to spindle-shaped bipolar neurons with small somas and rarely branched (A) and multipolar neurons with large somas (G). In both groups of neurons the cellular distribution of SK3 closely corresponded to that of the dopaminergic marker TH (B, H) and was found along the somata and dendrites (G displays examples of this distribution of staining). Merged color images show a high degree of colocalization (yellow) of SK3 (A, G, red) and TH (B, H, green). Many TH-positive neurons (E) show no expression of SK3 channel (D, F). Scale bar = 20 μm (See also Fig. S1).

using a short depolarizing voltage steps to elicit depolarization-activated outward tail currents displaying fast onset, small peak and fast decay time constant (Fig. 2A) characteristic of DN (Wolfart et al., 2001). I_{AHP} time-to-peak was 2–3 ms after the voltage step (Fig. 2A), and peak amplitudes were normally distributed (mean = 72 ± 4 pA; n = 31) (Fig. 2A inset). I_{AHP} decay time constant was markedly monoexponential (mean = 27 ± 0.5 ms, n = 31) (Fig. 2A) indicating that these neurons express a stereotypical set of ion channels mediating this current. No significant changes were found in time to peak, peak current or decay time constant at different holding potentials from −40 mV to −60 mV (data not shown). The current was blocked by external application of non-specific inhibitors of potassium channels (2 mM 4-AP and 20 mM TEA) (5 ± 3 pA, n = 5; $p < 0.01$) (Fig. 2B), while it was relatively insensitive to TEA 1–10 mM alone (data not shown). Removal of extracellular calcium almost completely abolished the I_{AHP} (13 ± 2 pA, n = 6; $p < 0.01$) (Fig. 2B). The outward tail current diminished in amplitude as holding potential was shifted to more negative values from −60 mV to −90 mV. I_{AHP} had a mean reversal potentials of −69 ± 5 mV; n = 6, (Fig. 2C), which is close to the theoretical potassium reversal potential for the solutions used (see Section 2.3).

Taken together, the fast onset, apparent voltage-insensitivity, calcium-dependence, differential sensitivities to broad-spectrum potassium channel blockers and reversal potential of the current elicited strongly suggest a calcium-dependent, potassium channel-mediated current. However, its relatively small maximum amplitude and fast decay time constant do not conclusively exclude involvement of other channels. On the other hand, I_{AHP} decays with a time course dependent on the amount of calcium influx, which depends upon the stimulation protocol (Sah, 1992), type of intracellular anion used in the intracellular solution (Zhang et al., 1994) and calcium-buffering capacity of the studied cell (Sah, 1992). Low $[Ca^{++}]_i$ accelerates the decay time constant (Sah, 1992; Zhang et al., 1994). We used an intracellular pipette solution with low calcium-buffering capacity to minimize non-physiological calcium buffering in the AMPA experiments (see Section 2.3). The simplest explanation for differences with published data in the peak current and decay time is that they reflect variations in the solutions used. Alternatively, these findings might suggest that SK channels have different assemblies from the SK channel isoforms reported in adult DN.

3.3. Channels underlying I_{AHP} have small unitary conductances

We analyzed current fluctuations to estimate channel properties taking advantage of the good signal-to-noise ratio obtained using whole-cell recordings (Hille, 2001). Unitary conductances of I_{AHP} channels were determined using variance–mean analysis (Fig. 3, see Section 2.3.1.1). Subtraction of the smoothed average (I_{mean}) (Fig. S2A) from 15 to 30 individual records (Fig. S2B) revealed increased variance (σ^2) during the outward tail current, which closely followed the time course of I_{AHP} (Fig. S2C). A plot of σ^2 to I_{mean} over the corresponding time segments yielded a relationship that could be well fitted with Eq. (1) (Fig. 2D) (see Section 2.3.1.1). From such plots we obtained estimates of single-channel current (i) and of maximum number of I_{AHP} channels (N) in DN. In 7 DN,

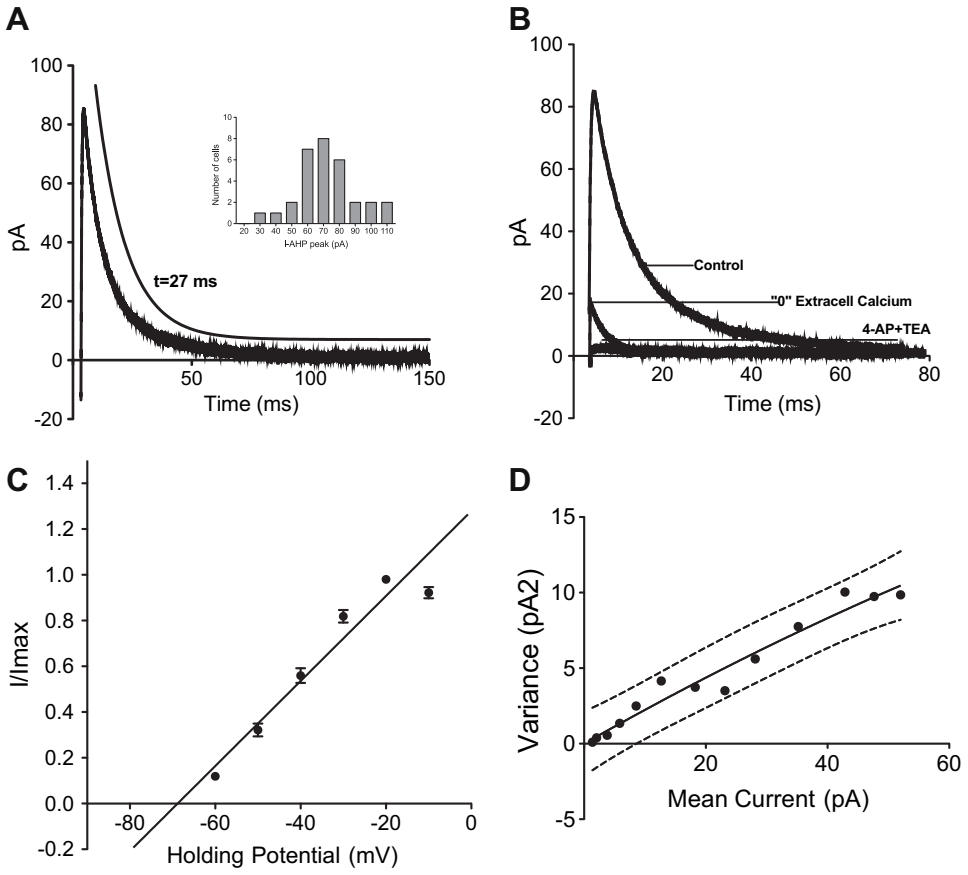

Fig. 2. Electrophysiological profile and I_{AHPs} in cultured embryonic rat ventral mesencephalon neurons. A, Whole-cell somatic voltage-clamp recording of an I_{AHP}. Distribution of I_{AHP} is well described by a single Gaussian function (inset; $n = 31$; $p > 0.10$, K–S normality test). The time constant of decay (in ms) was fitted between 90 and 10% of peak using a monoexponential function. B, Removal of extracellular calcium (0 Ca) reversibly reduced I_{AHP} amplitude ($n = 6$). I_{AHP} was completely blocked by specific blockers of potassium channels (2 mM 4-AP and 20 mM TEA) (lower). C, The ratio I (peak current amplitude)/I max (maximum current) is plotted against voltage (holding potential) (mean ± SEM; $n = 10$). D, Mean–variance analysis of the I_{AHP}. σ^2 of each of 13 current bins of the difference current is plotted as a function of I_{mean} of the corresponding bin (see Section 2.3.1.1). Dashed lines represent 95% confidence intervals. Solid line represents the best-fit curve. (See also Fig. S2).

unitary currents at −60 mV averaged 0.22 ± 0.3 pA, and N was estimated at 2007 ± 138 channels (Table 1). Using the estimated reversal potential in Fig. 2D, these results yield a unitary conductance for I_{AHP} channels of 20.6 ± 5 pS. These findings are in complete agreement with conductance values reported for SK channels (Vergara et al., 1998).

3.4. mAHP currents in cultured DN are apamin and 1-EBIO-sensitive

In most cell types SK channel-mediated I_{AHP} are specifically sensitive to apamin and 1-EBIO (Stocker, 2004; Pedarzani et al., 2005). Apamin is a bee venom toxin, which is a highly specific SK channel blocker with potencies in the low nanomolar range (Stocker, 2004) and 1-EBIO is the prototype agonist of SK channel (Pedarzani et al., 2005). Apamin (100 nM) reduced peak currents (33 ± 2 pA; $n = 11$; $p < 0.05$ vs. controls), time to rise (0.45 ± 0.1 ms; $n = 11$; $p < 0.05$), decay time (11.7 ± 1 ms; $n = 11$; $p < 0.05$), and charge transfer (207.7 ± 3 pC; $n = 11$; $p < 0.05$) (Fig. 3A, B). Conversely, 1-EBIO (100 μM) increased tail current amplitude by a factor of 1.48 (113.5 ± 4 pA; $n = 7$; $p < 0.01$ vs. controls), time to rise (1.01 ± 0.3 ms; $n = 7$; $p < 0.05$), decay time (55.5 ± 7 ms; $n = 7$; $p < 0.05$) and charge transfer (2240 ± 10 pC; $n = 7$; $p < 0.001$) of the same current (Fig. 3A, B). This pharmacological profile strongly supports a central role of SK3 channels on the I_{AHP} current.

3.5. Stimulation of glutamatergic AMPA receptors in cultured DN reduces AHP currents by reducing the number of functional SK channels in the membrane

In light of evidence implicating the participation of outward potassium currents in mediating several forms of DN death (Liss et al., 2005; Chan et al., 2007), and particularly the role of SK channels in glutamate-induced excitotoxicity (Lee et al., 2003), we tested the hypothesis that protracted glutamatergic AMPA-receptor stimulation would result in suppression of I_{SK}, opening the door for sustained excitation.

After 2 h exposure to AMPA (100 μM), I_{AHP} amplitude in DN was reduced by 67 ± 3% (44.5 ± 3 pA; $n = 9$; $p < 0.01$ vs. controls) (Fig. 3A). AMPA pretreatment reduced time to rise (0.51 ± 0.2 ms; $n = 9$; $p < 0.05$), decay time constant (9.4 ± 1 ms; $n = 9$; $p < 0.05$) and charge transfer (242.3 ± 5 pC; $n = 9$; $p < 0.05$) of the current (Fig. 3B). As shown by fluctuation analysis, AMPA reduced the maximum amplitude of the I_{AHP} without changing the initial slope of the σ^2 to I_{mean} relationship (Fig. 3C); therefore, single-channel current (0.24 ± 0.4 pA) was not changed (Table 1). Accurate estimates of N require obtaining estimates of σ^2 at high probabilities of channel opening where the current variance begins to decrease with increasing current level (because of the parabolic σ^2–I_{mean} relationship). Extrapolation of the fitted curve to high values of I_{mean} showed that AMPA treatment deviated from the linearity found under control conditions. At high values, a bell-shaped σ^2–I_{mean} relationship was found (Fig. 3C). Taken together these

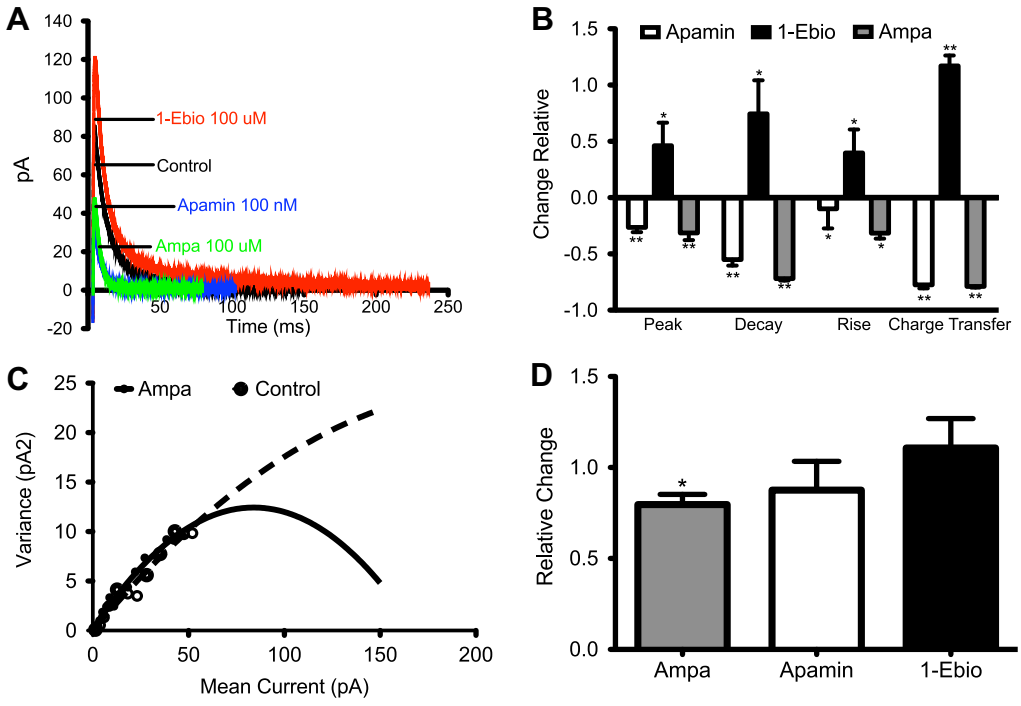

Fig. 3. Evoked I_{AHP} currents from cultured embryonic rat ventral mesencephalon neurons are apamin-, 1-EBIO- and AMPA-sensitive. A, The I_{AHP} was partially blocked by apamin (100 nM) and AMPA (100 μM) but enhanced by 1-EBIO (100 μM) applied to the bath. B, Bar diagram summarizing the effect of apamin (100 nM), AMPA (100 μM) and 1-EBIO (100 μM) on I_{AHP} peak amplitude, time to rise, decay time and charge transfer. Bars indicate normalized values with respective controls. *$p < 0.05$. C, Mean current to variance plot of I_{AHP} in controls cells (●) and cells exposed to 100 μM AMPA for 2 h (○). The variance of each of the 10–15 current bins (nonoverlapping intervals of 2 ms) of the difference current (each raw IAHP current was subtracted from the best-fitted polynomial curve) is plotted as a function of the arithmetic average mean current of the corresponding interval. Solid line (Controls) is the least-squares best fit to the equation described in Section 2.3.1.1 and gives a single-channel current of 0.22 ± 0.3 pA and an N of 2007 ± 138. The channel open probability at the peak current was 0.2–0.4. Dashed line (Ampa-treated) is the best fit for a single-channel current of 0.24 ± 0.4 pA and N of 669 ± 232. The channel open probability at the peak of the outward current was 0.22–0.32. (See also Fig. S2 and Table 1). D, Bar diagram summarizing the effect of apamin (100 nM), AMPA (100 μM) and 1-EBIO (100 μM) on the current density. Current density was calculated by dividing peak current by the capacitance. Bars indicate normalized values with respective controls. *$p < 0.05$.

results indicate a reduction in the number of functional channels in the membrane (Table 1).

In order to confirm the effect of AMPA on N, we used current density to test the relative change (Fig. 3D). DN had a membrane capacitance of 15.5 ± 0.8 pF ($n = 31$) and its relationship with peak current was linear (*Data not shown*). Current density was calculated dividing peak current by the capacitance. Current density in control DN was 5.74 ± 0.39 pA/pF ($n = 14$), and was significantly reduced by AMPA (100 μM) to 4.57 ± 0.32 pA/pF ($n = 9$; $p < 0.05$), but not changed by either apamin or 1-EBIO (Fig. 3D). These results strongly support a functional reduction in SK channel number in the membrane of AMPA-treated DN.

3.6. Selective AMPA toxicity to cultured DN is not additive to apamin toxicity

Experiments to test the neuroprotective potential of SK channel activation have provided contradictory results (Mourre et al., 1997; Salthun-Lassalle et al., 2004). Some have reported that inactivation of SK channels resulted in neurodegeneration (Mourre et al., 1997), while others reported increased neuronal excitability without ensuing neuronal death (Shakkottai et al., 2004), or even neuroprotection (Salthun-Lassalle et al., 2004). Conversely, administration of SK channel agonists *in vivo* increased the number of TH-positive cells in the midbrain after 6-hydroxy-dopamine injection (Aumann et al., 2008). We reported previously that exposure to AMPA results in concentration-dependent selective death of DN (de Erausquin et al., 2003, see also Fig. 4A), with commitment to die occurring as early as 2 h after onset of treatment (de Erausquin et al., 2003; Dorsey et al., 2006). To evaluate directly the involvement of SK channels in cellular defenses against excitotoxic insults in DN, we first analyzed the effects of blocking (apamin and NS8593) SK-mediated currents on survival of DN challenged with AMPA.

In cultures exposed for 12 h to 3–1000 nM apamin, the number of TH-positive neurons was reduced in a concentration-dependent manner relative to the number of TH-positive neurons counted in control cultures (Fig. 4B). The concentrations of apamin tested are in the functional range of SK antagonism in DN (Wolfart et al., 2001). Apamin 100 nM alone reduced survival to 76 ± 4.2% of controls ($p < 0.05$) (Fig. 4A); this concentration also significantly reduced I_{AHP} peaks (45% of controls, Fig. 3A). Examination of these cultures revealed a significant proportion of TH-positive neurons showing clear signs of degeneration (Figs. 5B9–12 and 6A3), reduction in soma size (Fig. 6D) and neurite pruning (Fig. 6A3, B). NS8593 is a new reversible inhibitor of SK3-mediated currents, which does not inhibit apamin binding but decreases calcium sensitivity of the channel by shifting the activation curve for Ca^{2+} to the right (Strobaek et al., 2006). NS8593

Table 1
Parameters estimated from variance–mean analysis. Mean–variance analysis of the I_{AHP} in cells treated with AMPA (100 μM) and apamin (100 nM). From Figs. 3 and 5 we obtained estimates of single-channel current (i) and of maximum number of I_{AHP} channels (N) in DN. Unitary conductance and maximum probability of opening were calculated taking into account Fig. 2 and Eq. (1). (See Section 2.3.1.1).

Treatment	Number of SK channels	Unitary current (pA)	Unitary conductance (pS)	Maximum probability of opening
Control	2007 ± 138	0.22 ± 0.3	20.6 ± 5	0.20–0.42
Apamin	1525 ± 250	0.19 ± 0.4	22.6 ± 6	0.11–0.22
AMPA	669 ± 232*	0.24 ± 0.4	24.2 ± 2	0.22–0.32

*$p < 0.05$.

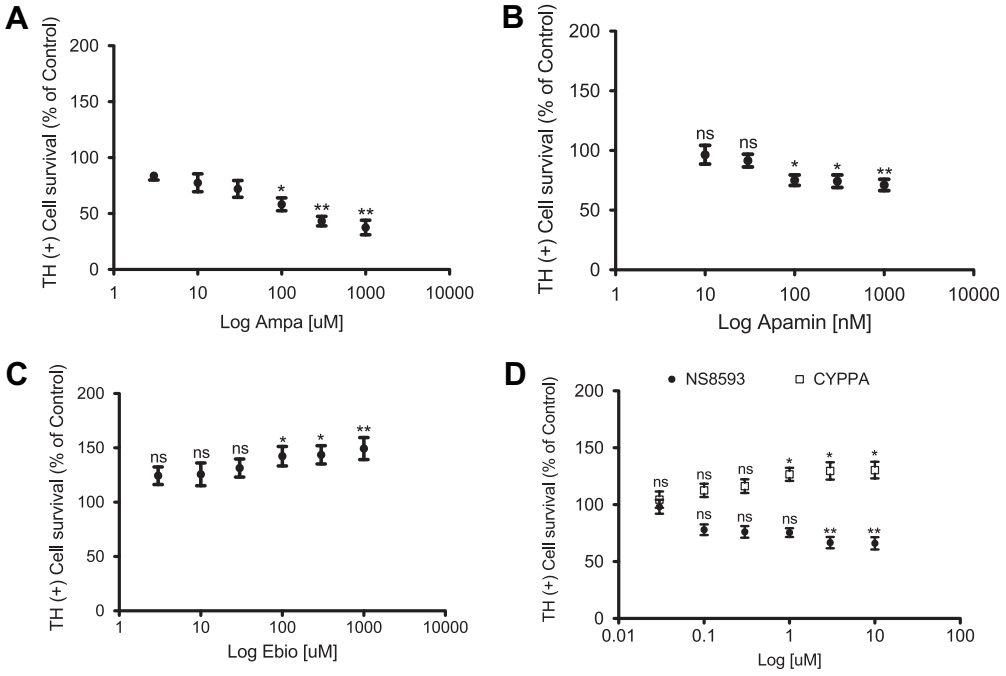

Fig. 4. Effect of AMPA, Apamin, 1-Ebio, NS8593 and CyPPA in the survival of cultured DN. A, AMPA concentration–response curve for TH-positive cells. DN were incubated with AMPA (3–1000 μM) for 12 h. B, Apamin concentration–response curve for TH-positive cells. DN were incubated with Apamin (3–1000 nM) for 12 h C, 1-EBIO concentration–response curve. DN were incubated with the SK channel activator, 1-EBIO (3–1000 μM) for 12 h. D, NS8593 and CyPPA concentration–response curve. DN were incubated with the SK channel activator, CyPPA or SK channel inhibitor, NS8593 (3–1000 μM) for 12 h. Survival is expressed as the percentage of cell loss after treatment. Data are expressed as mean ± SEM ($n = 6$).

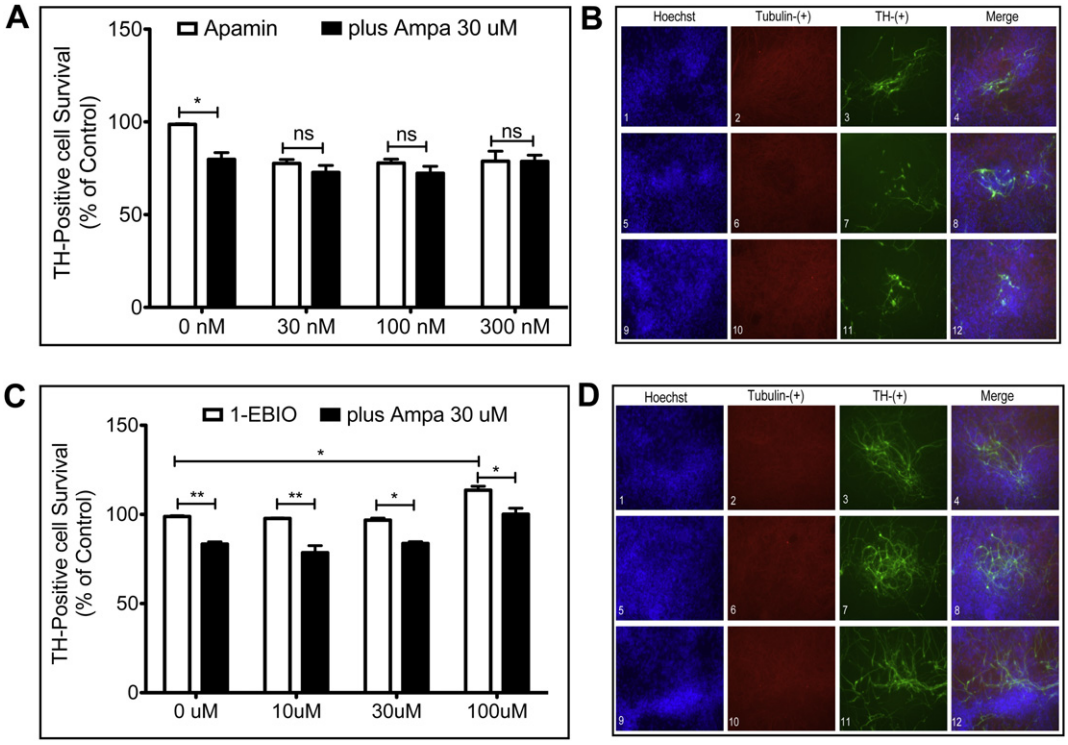

Fig. 5. AMPA-induced excitotoxicity in DN is not potentiated by Apamin and prevented by 1-Ebio. A, DN were incubated with the SK channel blocker, apamin (30–300 nM) for 12 h. Survival is expressed as the percentage of cell loss after treatment with apamin (30–300 nM) plus AMPA (30 μM). Data are expressed as mean ± SEM ($n = 6$). B, Representative photomicrographs of DN in (B1–4) untreated, (B5–8) apamin plus AMPA treated and (B9–12) apamin-treated cultures after 7 DIV. Scale bar = 20 μm. C, 1-EBIO concentration–response curve. DN were incubated with the SK channel activator, 1-EBIO (0–100 μM) and plus AMPA (30 μM) for 12 h. Data are expressed as mean ± SEM ($n = 3$). D, Representative photomicrographs of DN neurons in (D1–4) untreated, (D5–8) 1-EBIO plus AMPA treated, and (D9–12) EBIO-treated and cultures after 7 DIV.

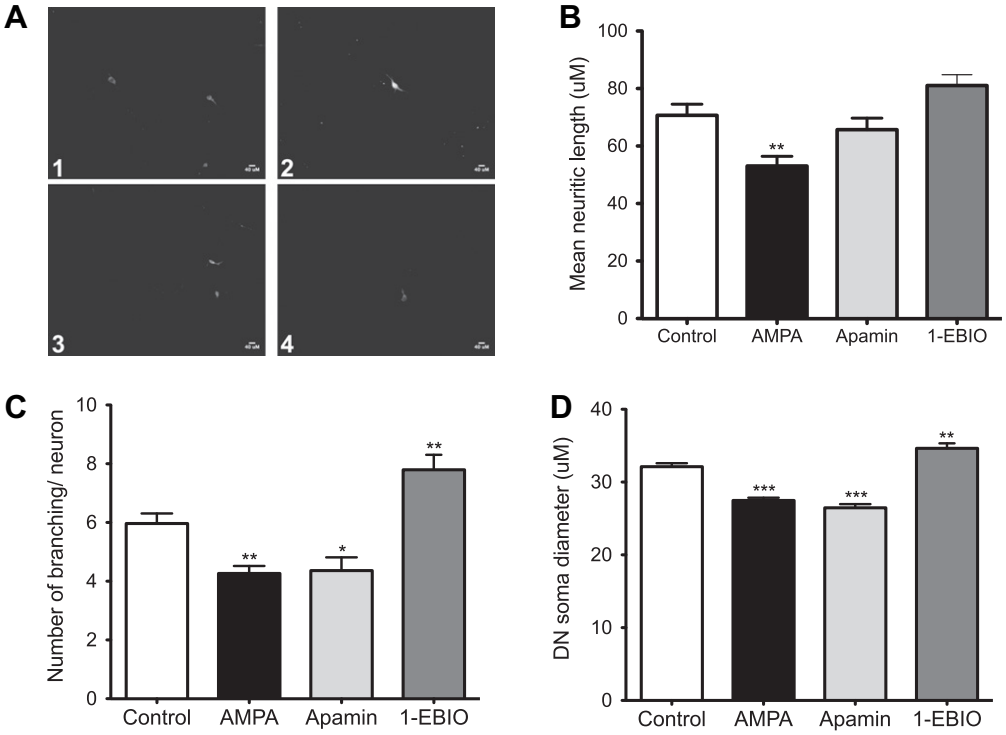

Fig. 6. Effects of SK in dendritic arborization of cultured DN. Representative photomicrographs of DN in (A1) untreated (A2) AMPA-treated (A3) apamin-treated and (A4) 1-EBIO-treated cultures after 7 DIV. Scale bar = 20 μm. Treatment of E14 ventral mesencephalon cultures with an SK blocker (apamin) or activator (1-Ebio) had significant effects on (B) total neurite length, (C) number of branches and (D) soma size in DN neurons. Data are expressed as mean ± SEM of measurements of 120 neurons in three independent experiments. ***$p < 0.001$ vs. untreated cultures. (See also Fig. S1).

also reduced the DN survival in a concentration-dependent manner (Fig. 4D).

Next, we evaluated the effect of a fixed concentration of AMPA known to cause selective degeneration of DN (30 μM) on the apamin concentration–response curve (30–300 nM) (Fig. 5A). The maximum effect of AMPA was not additive to apamin alone ($p > 0.05$), such that a ceiling effect was apparent for the combination. These results are consistent with a convergent pathway between excitotoxicity by AMPA and toxicity caused by SK blockade.

3.7. Activation of SK3 channels protects cultured DN against AMPA excitotoxicity

We next assessed the potential neuroprotective effect of SK3 channel activation in DN using 1-EBIO (Lee et al., 2003; Dolga et al., 2008). Exposure to 1-EBIO (30–1000 μM) alone for 12 h caused a significant reduction in spontaneous loss of DN (Fig. 4C) ($p < 0.01$, for 100 μM); at this concentration 1-EBIO significantly increased the I_{AHP} (134% of controls, Fig. 3A, B). 1-EBIO protected DN against AMPA-induced selective excitotoxicity in a concentration-dependent manner (Fig. 5C). Cell survival with 100 μM 1-EBIO plus AMPA 30 μM was 102.3 ± 3.8% ($p > 0.05$ vs. controls), while AMPA 30 μM alone resulted in 75.7 ± 5% survival ($p < 0.05$ vs. controls). TH-positive neurons rescued by 1-EBIO appeared healthier than control cells, showing larger neuritic trees ($p < 0.001$ vs. controls) and more branching points ($p < 0.01$ vs. controls) (Figs. 5D9–12 and 6A–D). CyPPA is a subtype-selective positive modulator of SK channels, which induces a leftward shift in the activation curves for calcium on SK3 and SK2 isoforms (Hougaard et al., 2007). CyPPA also prevented the normal cellular attrition of DN in culture (Fig. 4D).

4. Discussion

4.1. Phenotype-specific excitotoxicity in cultured DN

Prolonged exposure of mesencephalic primary cultures to AMPA resulted in a phenotype-specific toxicity to a subpopulation of DN (Figs. 4A and 6A–D). We have previously shown that the same treatment results in a trophic response in non-DN present in the same cultures (de Erausquin et al., 1994a, 2003; Isaacs et al., 1996). Since DN have a striking capacity for homeostatic regulation of synaptic inputs, which allows them to accommodate rapidly to maintained excitation and regain their baseline activity (Grace and Bunney, 2000), it appears that AMPA stimulation would have to overcome the intrinsic homeostatic system (e.g., via depolarization block) before causing toxicity. Previously, we established that in the same culture system sodium-based plasma membrane depolarization due to activation of AMPA receptors increases calcium influx through somatic L-type VDCC, which in turn produces a further rise in $[Ca^{++}]_i$ through mobilization of dantrolene-sensitive pools, leading to sustained loss of calcium homeostasis (de Erausquin et al., 1994a, 2003). We now show that AMPA also reduces I_{AHP} by ≈70% in DN (Fig. 3A), and affects all of the kinetic properties of SK currents (Fig. 3B). Our data strongly suggest that reduction of I_{AHP} precedes commitment to die because we have previously shown that release of cytochrome C (Cyt-C), activation of the transcription factor nuclear factor kappa B (NF-κβ) and p53-mediated neuronal death all require longer than 3 h of continuous exposure to AMPA (de Erausquin et al., 2003).

We have also shown previously that brief (5 min) exposures to AMPA induce sustained increases in the $[Ca^{++}]_i$ levels in DN, reaching approximately 300 nM (de Erausquin et al., 1994a), which is in the functional range of activation of SK channels (Stocker,

2004). We now found that after 120 min of AMPA exposure, I_{SK} is significant reduced (Fig. 3A, B). This biphasic cellular response has been previously reported in adult DN where mGluR1 stimulation induces short latency hyperpolarization followed by a significant depolarization, which is mediated by changes in $[Ca^{++}]_i$ and activation and inactivation of SK channels, respectively (Fiorillo and Williams, 1998). Different mechanisms could explain this phenomenon, including (*i*) reduction in calcium intracellular stores (Paladini et al., 2001), (*ii*) reduction in $[Ca^{++}]_i$ in the vicinity of SK channels (Augustine et al., 2003; Helmchen et al., 1996), (*iii*) desensitization of SK channels to calcium (Taylor et al., 2003; Allen et al., 2007). High $[Ca^{++}]_i$ levels also may block the channel in a voltage-dependent fashion and induce an inwardly rectifying SK current (Soh and Park, 2001). Similarly, sustained $[Ca^{++}]_i$ levels induced by AMPA (de Erausquin et al., 1994a) could desensitize or block SK channels. However, we found that unitary channel current is not affected by AMPA (Fig. 3C, Table 1), and therefore its effect has to be accounted for by either inactivation (Fig. 3C) or removal of channels from the membrane (Fig. 3C, D, Table 1). Interestingly, activation of dendritic AMPA receptors in DN decreases I_{AHP} independently of $[Ca^{++}]_i$ pools, transiently overwhelming the SK conductances (Blythe et al., 2007), which is in accordance with a reduction in SK3 channel number in the membrane due to protracted activation of AMPA receptors (Fig. 3C, D, Table 1). SK channels undergo recycling (Faber et al., 2008) and activation of cyclic AMP-dependent protein kinase (PKA) increases their endocytosis (Ren et al., 2006). However, in DN it has been shown that PKA activation did not regulate SK channel function or surface expression (Riegel and Williams, 2008), and fails to improve DN survival in AMPA-induced excitotoxicity (*data not shown*). Thus, the molecular mechanism of AMPA-induced reduction in the number of available channels remains to be elucidated. Notably, the SK3 promoter has putative binding sites for CREB (Sun et al., 2001) and NF-κβ (Kye et al., 2007), both of which we have shown to be regulated by AMPA in DN (de Erausquin et al., 1994a, 2003; Isaacs et al., 1996).

Selective excitotoxicity to DN by AMPA is characterized by cytosolic vacuolation, swelling of the Golgi apparatus and mitochondria, pruning of neurites, loss of presynaptic contacts, chromatin condensation, and nuclear invagination (Dorsey et al., 2006). These ultrastructural changes resemble those described in primary cortical cultures treated with apamin (Spoerri et al., 1975; Spoerri, 1983). In DN, SK3 channels (Wolfart et al., 2001, see also Fig. 1G) as well as AMPA receptors (de Erausquin et al., 1994a; Paquet et al., 1997) are expressed throughout the entire somatodendritic axis. The most immediate and profound morphological effects of AMPA (Fig. 6A2) and apamin (Fig. 6A3) are observed on dendrites (Fig. 6B), where both lead to selective retraction, beading and fragmentation (Fig. 6), while axons are consistently spared (Fig. S1B, C). In theoretical models of DN function, oscillatory frequency is inversely related to compartment diameter due to the clearance rate of $[Ca^{++}]_i$ (Kuznetsov et al., 2006). Thus, dendrite susceptibility may be due to large oscillations in $[Ca^{++}]_i$ generated by calcium-dependent pacemaking (Wilson and Callaway, 2000). In addition, loss of synaptic contacts and reduction in size and complexity of the dendritic tree resulting from AMPA excitotoxicity (de Erausquin et al., 2003) would further reduce synaptic input and restrict oscillations to the soma, where SK channels play a larger role (Kuznetsov et al., 2006; Wilson and Callaway, 2000). Thus, AMPA-induced suppression of I_{SK} would lead to high-frequency bursting (Blythe et al., 2007) in a positive feedback loop.

We found that the inactivation of SK channels by apamin (Figs. 4B, 5A, B9–12 and 6A2) or NS8593 (Fig. 4D) promotes specific death of DN sharing a convergent pathway with AMPA-induced excitotoxicity (Fig. 5A, B5–8). DN in the midbrain show differential binding affinity and electrophysiological response to apamin, making it possible to distinguish subtypes of DN based on apamin response (Gu et al., 1992), consistent with selective expression of SK channels (Wolfart et al., 2001, see also Fig. 1). Apamin prevented spontaneous attrition of cultured DN (Salthun-Lassalle et al., 2004), but at concentrations (500 μM) several orders of magnitude higher than the IC50 for blocking SK3-mediated I_{AHP} (100 nM) (Wolfart et al., 2001), suggesting that the molecular target of this effect may be different. Apamin-induced neurodegeneration may involve deregulation of $[Ca^{++}]_i$ (Mourre et al., 1997). Acute administration of apamin both *in vitro* and *in vivo* increases firing rate and burst firing in DN (Ji and Shepard, 2006; Wolfart et al., 2001), but when chronically administered it causes a less electrically active state associated with persistent depolarization (Aumann et al., 2008). Thus, it appears that SK channel inhibition by apamin overcomes the intrinsic homeostatic system before causing toxicity to DN.

1-EBIO promoted both survival (Figs. 4C and 5B, D9–12) and differentiation (Fig. 6A4) of cultured DN. These results are in agreement with activation of SK3 channels using 1-EBIO leads to an increase of neuritogenesis (Fig. 6B, C) (Liebau et al., 2007) and the overall expression level of SK3 channel increases with the synaptic maturation (Obermair et al., 2003). These findings clearly show that, in response to hyperexcitable conditions, DN may use I_{SK} homeostatically as a key but previously unrecognized protecting mechanism (de Erausquin, 2004). Similarly, the neuroprotective effects reported for riluzole in PD (LeWitt and Taylor, 2008) may be due to a very significant, rapid, stable, reversible and concentration-dependent stimulation of SK3 channels (Grunnet et al., 2001). The trophic effects of 1-EBIO (Fig. 6B, D) are likely explained by the rescue of DN that degenerate as a result of culture-related neuronal attrition (Fig. 5C). However, a recruitment of precursors not initially committed to the dopaminergic phenotype cannot be excluded, especially considering that it has been recently reported in an adult rodent model of PD *in vivo* that chronic activation of SK channel shifted the neurochemical phenotype of SNpc neurons from TH-negative to TH-positive (Aumann et al., 2008).

SK channels are ideally suited to transduce calcium mobilization central to excitotoxic injury into a protective, hyperpolarizing signal. Indeed, SK channel-mediated I_{AHP} contributes to the refractory period (Stocker, 2004), and potentiation of the I_{AHP} by cytosolic calcium would certainly dampen excitability. Our results suggest that persistent activation of SK channels caused by 1-EBIO or CyPPA (Fig. 4D) might tonically hyperpolarize DN reducing their spontaneous activity, regularizing their firing pattern and reducing metabolic demands and oxidative stress. However, it has been reported that a subgroup of DN are highly vulnerable to changes in electrical activity, such that activation of ATP-sensitive potassium channels results in neurodegeneration (Liss et al., 2005). Thus, differences in the effect of SK regulation on survival of DN may be accounted for by different molecular phenotypes. In the more general case, 1-EBIO or CyPPA would cause a permissive environment to maintain and facilitate SK3-mediated DA survival (Fig. 6D9–12). The activation of SK channels by 1-EBIO or CyPPA has shown promising features as a classic neuroprotectant for DN including antiexcitotoxic, antiapoptotic, antioxidant and pro-metabolic actions.

Here we have demonstrated that SK channel inhibition is a functionally defined candidate mechanism for differential vulnerability of DA midbrain neurons to AMPA-induced neurotoxicity prior to commitment to die.

Acknowledgements

The authors wish to thank Dr. Steve Mennerick for help setting up the electrophysiology experiments. We also want to

acknowledge our debt of gratitude to the late Dr. Erminio Costa, without whose mentorship, encouragement, and inspiration this work would not have been possible. This work was supported by NIMH K08MH077220 award to GdE, and by NIH Neuroscience Blueprint Interdisciplinary Center Core Grant P30 NS057105 to Washington University, Washington University Department of Psychiatry Fund #93785, and Brigham and Women's Hospital Department of Psychiatry Fund #016507.

Appendix. Supplementary material

Supplementary data related to this article can be found online at doi:10.1016/j.neuropharm.2010.10.024.

References

Alavian, K.N., Scholz, C., Simon, H.H., 2008. Transcriptional regulation of mesencephalic dopaminergic neurons: the full circle of life and death. Movement Disorders: Official Journal of the Movement Disorder Society 23, 319–328.

Allen, D., Fakler, B., Maylie, J., Adelman, J.P., 2007. Organization and regulation of small conductance Ca^{2+}-activated K^+ channel multiprotein complexes. The Journal of Neuroscience: The Official Journal of the Society for Neuroscience 27, 2369–2376.

Augustine, G.J., Santamaria, F., Tanaka, K., 2003. Local calcium signaling in neurons. Neuron 40, 331–346.

Aumann, T.D., Gantois, I., Egan, K., Vais, A., Tomas, D., Drago, J., Horne, M.K., 2008. SK channel function regulates the dopamine phenotype of neurons in the substantia nigra pars compacta. Experimental Neurology 213, 419–430.

Beckstead, M.J., Grandy, D.K., Wickman, K., Williams, J.T., 2004. Vesicular dopamine release elicits an inhibitory postsynaptic current in midbrain dopamine neurons. Neuron 42, 939–946.

Blythe, S.N., Atherton, J.F., Bevan, M.D., 2007. Synaptic activation of dendritic AMPA and NMDA receptors generates transient high-frequency firing in substantia nigra dopamine neurons in vitro. Journal of Neurophysiology 97, 2837–2850.

Bond, C.T., Herson, P.S., Strassmaier, T., Hammond, R., Stackman, R., Maylie, J., Adelman, J.P., 2004. Small conductance Ca^{2+}-activated K^+ channel knock-out mice reveal the identity of calcium-dependent afterhyperpolarization currents. The Journal of Neuroscience: The Official Journal of the Society for Neuroscience 24, 5301–5306.

Branton, R.L., Clarke, D.J., 1999. Apoptosis in primary cultures of E14 rat ventral mesencephala: time course of dopaminergic cell death and implications for neural transplantation. Experimental Neurology 160, 88–98.

Burke, R.E., 2004. Ontogenic cell death in the nigrostriatal system. Cell and Tissue Research 318, 63–72.

Chan, C.S., Guzman, J.N., Ilijic, E., Mercer, J.N., Rick, C., Tkatch, T., Meredith, G.E., Surmeier, D.J., 2007. 'Rejuvenation' protects neurons in mouse models of Parkinson's disease. Nature 447, 1081–1086.

Chiodo, L.A., Kapatos, G., 1992. Membrane properties of identified mesencephalic dopamine neurons in primary dissociated cell culture. Synapse (New York, N.Y.) 11, 294–309.

Damier, P., Hirsch, E.C., Agid, Y., Graybiel, A.M., 1999. The substantia nigra of the human brain. II. Patterns of loss of dopamine-containing neurons in Parkinson's disease. Brain: A Journal of Neurology 122 (Pt 8), 1437–1448.

Dauer, W., Przedborski, S., 2003. Parkinson's disease: mechanisms and models. Neuron 39, 889–909.

de Erausquin, G., Brooker, G., Costa, E., Hanbauer, I., 1994a. Persistent AMPA receptor stimulation alters $[Ca^{2+}]_i$ homeostasis in cultures of embryonic dopaminergic neurons. Brain Research. Molecular Brain Research 21, 303–311.

de Erausquin, G.A., Costa, E., Hanbauer, I., 1994b. Calcium homeostasis, free radical formation, and trophic factor dependence mechanisms in Parkinson's disease. Pharmacological Reviews 46, 467–482.

de Erausquin, G.A., Hanbauer, I., 1995. AMPA receptor-induced dopaminergic cell death: a model for the pathogenesis of hypofrontality and negative symptoms in schizophrenia. In: Mednick, S.A., Hollister, J.M. (Eds.), Neural Development and Schizophrenia. Plenum Press, NY.

de Erausquin, G.A., Hyrc, K., Dorsey, D.A., et al., 2003. Nuclear translocation of nuclear transcription factor-kappa B by alpha-amino-3-hydroxy-5-methyl-4-isoxazolepropionic acid receptors leads to transcription of p53 and cell death in dopaminergic neurons. Molecular Pharmacology 63, 784–790.

de Erausquin, G.A., 2004. Transactivation of cell death signals by glutamate transmission in dopaminergic neurons. Critical Reviews in Neurobiology 16, 107–119.

Dolga, A.M., Granic, I., Blank, T., Knaus, H.G., Spiess, J., Luiten, P.G., Eisel, U.L., Nijholt, I.M., 2008. TNF-alpha-mediates neuroprotection against glutamate-induced excitotoxicity via NF-kappaB-dependent up-regulation of K2.2 channels. Journal of Neurochemistry 107, 1158–1167.

Dorsey, D.A., Masco, D.H., Dikranian, K., Hyrc, K., Masciotra, L., Faddis, B., Soriano, M., Gru, A.A., Goldberg, M.P., de Erausquin, G.A., 2006. Ultrastructural characterization of alpha-amino-3-hydroxy-5-methyl-4-isoxazolepropionic acid-induced cell death in embryonic dopaminergic neurons. Apoptosis: An International Journal on Programmed Cell Death 11, 535–544.

Faber, E.S., Delaney, A.J., Power, J.M., Sedlak, P.L., Crane, J.W., Sah, P., 2008. Modulation of SK channel trafficking by beta adrenoceptors enhances excitatory synaptic transmission and plasticity in the amygdala. The Journal of Neuroscience: The Official Journal of the Society for Neuroscience 28, 10803–10813.

Fakler, B., Adelman, J.P., 2008. Control of K(ca) channels by calcium nano/microdomains. Neuron 59, 873–881.

Falkenburger, B.H., Schulz, J.B., 2006. Limitations of cellular models in Parkinson's disease research. Journal of Neural Transmission. Supplementum 70, 261–268.

Fiorillo, C.D., Williams, J.T., 1998. Glutamate mediates an inhibitory postsynaptic potential in dopamine neurons. Nature 394, 78–82.

Garduno, J., Galvan, E., Fernandez de Sevilla, D., Buno, W., 2005. 1-Ethyl-2-benzimidazolinone (EBIO) suppresses epileptiform activity in in vitro hippocampus. Neuropharmacology 49, 376–388.

Grace, A.A., Bunney, B.S., 2000. Electrophysiological properties of midbrain dopamine neuron. In: Bloom, F.E., Kupfer, D.J. (Eds.), Psychopharmacology: the Fourth Generation of Progress, fourth ed. ACNP, US.

Greco, D., Volpicelli, F., Di Lieto, A., Leo, D., Perrone-Capano, C., Auvinen, P., di Porzio, U., 2009. Comparison of gene expression profile in embryonic mesencephalon and neuronal primary cultures. PloS One 4, e4977.

Grunnet, M., Jespersen, T., Angelo, K., Frokjaer-Jensen, C., Klaerke, D.A., Olesen, S.P., Jensen, B.S., 2001. Pharmacological modulation of SK3 channels. Neuropharmacology 40, 879–887.

Gu, X., Blatz, A.L., German, D.C., 1992. Subtypes of substantia nigra dopaminergic neurons revealed by apamin: autoradiographic and electrophysiological studies. Brain Research Bulletin 28, 435–440.

Harrison, P.J., Weinberger, D.R., 2005. Schizophrenia genes, gene expression, and neuropathology: on the matter of their convergence. Molecular Psychiatry 10, 40–68. image 5.

Heinemann, S.H., Conti, F., 1992. Nonstationary noise analysis and application to patch clamp recordings. Methods in Enzymology 207, 131–148.

Helmchen, F., Imoto, K., Sakmann, B., 1996. Ca^{2+} buffering and action potential-evoked Ca^{2+} signaling in dendrites of pyramidal neurons. Biophysical Journal 70, 1069–1081.

Hille, B., 2001. Ion Channels of Excitable Membranes. Sinauer Associates, USA.

Hougaard, C., Eriksen, B.L., Jorgensen, S., Johansen, T.H., Dyhring, T., Madsen, L.S., Strobaek, D., Christophersen, P., 2007. Selective positive modulation of the SK3 and SK2 subtypes of small conductance Ca^{2+}-activated K^+ channels. British Journal of Pharmacology 151, 655–665.

Isaacs, K.R., de Erausquin, G., Strauss, K.I., Jacobowitz, D.M., Hanbauer, I., 1996. Differential effects of excitatory amino acids on mesencephalic neurons expressing either calretinin or tyrosine hydroxylase in primary cultures. Brain Research. Molecular Brain Research 36, 114–126.

Ji, H., Shepard, P.D., 2006. SK Ca^{2+}-activated K^+ channel ligands alter the firing pattern of dopamine-containing neurons in vivo. Neuroscience 140, 623–633.

Kobayashi, K., Nishizawa, Y., Sawada, K., Ogura, H., Miyabe, M., 2008. K(+)-channel openers suppress epileptiform activities induced by 4-aminopyridine in cultured rat hippocampal neurons. Journal of Pharmacological Sciences 108, 517–528.

Kuznetsov, A.S., Kopell, N.J., Wilson, C.J., 2006. Transient high-frequency firing in a coupled-oscillator model of the mesencephalic dopaminergic neuron. Journal of Neurophysiology 95, 932–947.

Kye, M.J., Spiess, J., Blank, T., 2007. Transcriptional regulation of intronic calcium-activated potassium channel SK2 promoters by nuclear factor-kappa B and glucocorticoids. Molecular and Cellular Biochemistry 300, 9–17.

Lappin, S.C., Dale, T.J., Brown, J.T., Trezise, D.J., Davies, C.H., 2005. Activation of SK channels inhibits epileptiform bursting in hippocampal CA3 neurons. Brain Research 1065, 37–46.

Lee, A.L., Dumas, T.C., Tarapore, P.E., Webster, B.R., Ho, D.Y., Kaufer, D., Sapolsky, R.M., 2003. Potassium channel gene therapy can prevent neuron death resulting from necrotic and apoptotic insults. Journal of Neurochemistry 86, 1079–1088.

LeWitt, P.A., Taylor, D.C., 2008. Protection against Parkinson's disease progression: clinical experience. Neurotherapeutics: The Journal of the American Society for Experimental NeuroTherapeutics 5, 210–225.

Licker, V., Kövari, E., Hochstrasser, D.F., Burkhard, P.R., 2009. Proteomics in human Parkinson's disease research. Journal of Proteomics 73, 10–29.

Liebau, S., Vaida, B., Proepper, C., Grissmer, S., Storch, A., Boeckers, T.M., Dietl, P., Wittekindt, O.H., 2007. Formation of cellular projections in neural progenitor cells depends on SK3 channel activity. Journal of Neurochemistry 101, 1338–1350.

Lilliu, V., Pernas-Alonso, R., Trelles, R.D., di Porzio, U., Zuddas, A., Perrone-Capano, C., 2001. Ontogeny of AMPA receptor gene expression in the developing rat midbrain and striatum. Brain Research. Molecular Brain Research 96, 133–141.

Liss, B., Franz, O., Sewing, S., Bruns, R., Neuhoff, H., Roeper, J., 2001. Tuning pacemaker frequency of individual dopaminergic neurons by Kv4.3L and KChip3.1 transcription. The EMBO Journal 20, 5715–5724.

Liss, B., Haeckel, O., Wildmann, J., Miki, T., Seino, S., Roeper, J., 2005. K-ATP channels promote the differential degeneration of dopaminergic midbrain neurons. Nature Neuroscience 8, 1742–1751.

Liss, B., Roeper, J., 2008. Individual dopamine midbrain neurons: functional diversity and flexibility in health and disease. Brain Research Reviews 58, 314–321.

Marani, E., Heida, T., Lakke, E.A., Usunoff, K.G., 2008. The subthalamic nucleus. Part I: development, cytology, topography and connections. Advances in Anatomy, Embryology, and Cell Biology 198, 1–113. vii.

Michel, P.P., Alvarez-Fischer, D., Guerreiro, S., Hild, A., Hartmann, A., Hirsch, E.C., 2007. Role of activity-dependent mechanisms in the control of dopaminergic neuron survival. Journal of Neurochemistry 101, 289–297.

Moore, D.J., West, A.B., Dawson, V.L., Dawson, T.M., 2005. Molecular pathophysiology of Parkinson's disease. Annual Review of Neuroscience 28, 57–87.

Mourre, C., Fournier, C., Soumireu-Mourat, B., 1997. Apamin, a blocker of the calcium-activated potassium channel, induces neurodegeneration of Purkinje cells exclusively. Brain Research 778, 405–408.

Neuhoff, H., Neu, A., Liss, B., Roeper, J., 2002. I(h) channels contribute to the different functional properties of identified dopaminergic subpopulations in the midbrain. The Journal of Neuroscience: The Official Journal of the Society for Neuroscience 22, 1290–1302.

Obermair, G.J., Kaufmann, W.A., Knaus, H.G., Flucher, B.E., 2003. The small conductance Ca^{2+}-activated K^+ channel SK3 is localized in nerve terminals of excitatory synapses of cultured mouse hippocampal neurons. The European Journal of Neuroscience 17, 721–731.

Paladini, C.A., Fiorillo, C.D., Morikawa, H., Williams, J.T., 2001. Amphetamine selectively blocks inhibitory glutamate transmission in dopamine neurons. Nature Neuroscience 4, 275–281.

Paquet, M., Tremblay, M., Soghomonian, J.J., Smith, Y., 1997. AMPA and NMDA glutamate receptor subunits in midbrain dopaminergic neurons in the squirrel monkey: an immunohistochemical and in situ hybridization study. The Journal of Neuroscience: The Official Journal of the Society for Neuroscience 17, 1377–1396.

Pedarzani, P., McCutcheon, J.E., Rogge, G., Jensen, B.S., Christophersen, P., Hougaard, C., Strobaek, D., Stocker, M., 2005. Specific enhancement of SK channel activity selectively potentiates the afterhyperpolarizing current I(AHP) and modulates the firing properties of hippocampal pyramidal neurons. The Journal of Biological Chemistry 280, 41404–41411.

Puopolo, M., Raviola, E., Bean, B.P., 2007. Roles of subthreshold calcium current and sodium current in spontaneous firing of mouse midbrain dopamine neurons. The Journal of Neuroscience: The Official Journal of the Society for Neuroscience 27, 645–656.

Ren, Y., Barnwell, L.F., Alexander, J.C., Lubin, F.D., Adelman, J.P., Pfaffinger, P.J., Schrader, L.A., Anderson, A.E., 2006. Regulation of surface localization of the small conductance Ca^{2+}-activated potassium channel, Sk2, through direct phosphorylation by cAMP-dependent protein kinase. The Journal of Biological Chemistry 281, 11769–11779.

Riegel, A.C., Williams, J.T., 2008. CRF facilitates calcium release from intracellular stores in midbrain dopamine neurons. Neuron 57, 559–570.

Sah, P., 1992. Role of calcium influx and buffering in the kinetics of Ca(2+)-activated K^+ current in rat vagal motoneurons. Journal of Neurophysiology 68, 2237–2247.

Sah, P., Isaacson, J.S., 1995. Channels underlying the slow afterhyperpolarization in hippocampal pyramidal neurons: neurotransmitters modulate the open probability. Neuron 15, 435–441.

Salthun-Lassalle, B., Hirsch, E.C., Wolfart, J., Ruberg, M., Michel, P.P., 2004. Rescue of mesencephalic dopaminergic neurons in culture by low-level stimulation of voltage-gated sodium channels. The Journal of Neuroscience: The Official Journal of the Society for Neuroscience 24, 5922–5930.

Sapolsky, R.M., 2001. Cellular defenses against excitotoxic insults. Journal of Neurochemistry 76, 1601–1611.

Sarpal, D., Koenig, J.I., Adelman, J.P., Brady, D., Prendeville, L.C., Shepard, P.D., 2004. Regional distribution of SK3 mRNA-containing neurons in the adult and adolescent rat ventral midbrain and their relationship to dopamine-containing cells. Synapse (New York, N.Y.) 53, 104–113.

Seutin, V., Massotte, L., Renette, M.F., Dresse, A., 2001. Evidence for a modulatory role of ih on the firing of a subgroup of midbrain dopamine neurons. Neuroreport 12, 255–258.

Shakkottai, V.G., Chou, C.H., Oddo, S., Sailer, C.A., Knaus, H.G., Gutman, G.A., Barish, M.E., LaFerla, F.M., Chandy, K.G., 2004. Enhanced neuronal excitability in the absence of neurodegeneration induces cerebellar ataxia. The Journal of Clinical Investigation 113, 582–590.

Sigworth, F.J., 1980. The conductance of sodium channels under conditions of reduced current at the node of Ranvier. The Journal of Physiology 307, 131–142.

Silva, N.L., Pechura, C.M., Barker, J.L., 1990. Postnatal rat nigrostriatal dopaminergic neurons exhibit five types of potassium conductances. Journal of Neurophysiology 64, 262–272.

Soh, H., Park, C.S., 2001. Inwardly rectifying current-voltage relationship of small-conductance Ca^{2+}-activated K^+ channels rendered by intracellular divalent cation blockade. Biophysical Journal 80, 2207–2215.

Spoerri, P.E., Jentsch, J., Glees, P., 1975. Apamin from bee venom. effects of the neurotoxin on subcellular particles of neural cultures. FEBS Letters 53, 143–147.

Spoerri, P.E., 1983. Changes induced by apamin from bee venom on differentiated mouse neuroblastoma cells in culture. Acta Anatomica 117, 346–354.

Stocker, M., Pedarzani, P., 2000. Differential distribution of three Ca(2+)-activated K(+) channel subunits, SK1, SK2, and SK3, in the adult rat central nervous system. Molecular and Cellular Neurosciences 15, 476–493.

Stocker, M., 2004. Ca(2+)-activated K^+ channels: molecular determinants and function of the SK family. Nature Reviews. Neuroscience 5, 758–770.

Strobaek, D., Hougaard, C., Johansen, T.H., Sorensen, U.S., Nielsen, E.O., Nielsen, K.S., Taylor, R.D., Pedarzani, P., Christophersen, P., 2006. Inhibitory gating modulation of small conductance Ca^{2+}-activated K^+ channels by the synthetic compound (R)-N-(benzimidazol-2-yl)-1,2,3,4-tetrahydro-1-naphtylamine (NS8593) reduces afterhyperpolarizing current in hippocampal CA1 neurons. Molecular Pharmacology 70, 1771–1782.

Sun, G., Tomita, H., Shakkottai, V.G., Gargus, J.J., 2001. Genomic organization and promoter analysis of human KCNN3 gene. Journal of Human Genetics 46, 463–470.

Tacconi, S., Carletti, R., Bunnemann, B., Plumpton, C., Merlo Pich, E., Terstappen, G.C., 2001. Distribution of the messenger RNA for the small conductance calcium-activated potassium channel SK3 in the adult rat brain and correlation with immunoreactivity. Neuroscience 102, 209–215.

Tanabe, M., Mori, M., Gahwiler, B.H., Gerber, U., 1999. Apamin-sensitive conductance mediates the K(+) current response during chemical ischemia in CA3 pyramidal cells. Journal of Neurophysiology 82, 2876–2882.

Taylor, M.S., Bonev, A.D., Gross, T.P., Eckman, D.M., Brayden, J.E., Bond, C.T., Adelman, J.P., Nelson, M.T., 2003. Altered expression of small-conductance Ca^{2+}-activated K^+ (SK3) channels modulates arterial tone and blood pressure. Circulation Research 93, 124–131.

Valiante, T.A., Abdul-Ghani, M.A., Carlen, P.L., Pennefather, P., 1997. Analysis of current fluctuations during after-hyperpolarization current in dentate granule neurones of the rat hippocampus. The Journal of Physiology 499 (Pt 1), 121–134.

Vergara, C., Latorre, R., Marrion, N.V., Adelman, J.P., 1998. Calcium-activated potassium channels. Current Opinion in Neurobiology 8, 321–329.

Vogalis, F., Furness, J.B., Kunze, W.A., 2001. Afterhyperpolarization current in myenteric neurons of the guinea pig duodenum. Journal of Neurophysiology 85, 1941–1951.

Wilson, C.J., Callaway, J.C., 2000. Coupled oscillator model of the dopaminergic neuron of the substantia nigra. Journal of Neurophysiology 83, 3084–3100.

Wolfart, J., Neuhoff, H., Franz, O., Roeper, J., 2001. Differential expression of the small-conductance, calcium-activated potassium channel SK3 is critical for pacemaker control in dopaminergic midbrain neurons. The Journal of Neuroscience: The Official Journal of the Society for Neuroscience 21, 3443–3456.

Yang, C.R., Seamans, J.K., Gorelova, N., 1999. Developing a neuronal model for the pathophysiology of schizophrenia based on the nature of electrophysiological actions of dopamine in the prefrontal cortex. Neuropsychopharmacology: Official Publication of the American College of Neuropsychopharmacology 21, 161–194.

Zhang, L., Weiner, J.L., Valiante, T.A., Velumian, A.A., Watson, P.L., Jahromi, S.S., Schertzer, S., Pennefather, P., Carlen, P.L., 1994. Whole-cell recording of the Ca(2+)-dependent slow afterhyperpolarization in hippocampal neurones: effects of internally applied anions. Pflugers Archiv: European Journal of Physiology 426, 247–253.